Applied Computer Science 2025, vol. 21, no. 1, pp. 31–43
https://doi.org/10.35784/acs_6902

Submitted: 2024-12-04 | Revised: 2025-01-29 | Accepted: 2025-02-01

Keywords: pipeline,numerical modeling, internal pressure,longitudinal crack, XFEM

Aya BARKAOUI [1*], *Mohammed EL MOUSSAID* [2], *Hassane MOUSTABCHIR* [1]
[1] National School of Applied Sciences, Morocco, aya.barkaoui@usmba.ac.ma, hassane.moustabchir@usmba.ac.ma
[2] S3I Research Center, Morocco, mohammed.elmoussaid@artsetmetiers.ma
[*] Corresponding author: aya.barkaoui@usmba.ac.ma

Numerical modelling and comparison of SIF in pipelines exposed to internal pressure with longitudinal crack using XFEM method

Abstract

This study investigates the feasibility of using the extended finite element method (XFEM) in the ABAQUS commercial software, employing the maximum principal stress as the damage parameter. The primary objective of this work is to calculate the mode I stress intensity factor, a key parameter for understanding the crack initiation mechanisms in pressurized pipelines. Initially, an analysis of Von Mises stresses was conducted, followed by a theoretical calculation of stress intensity factors based on analytical methods from the literature. The results were compared with those obtained from numerical simulations using XFEM. Validation of the findings was also carried out by benchmarking them against previous studies employing the classical finite element method (FEM). Additionally, various parameters, such as internal pressure and initial crack length, were examined to assess their impact on the fatigue behavior of the structure. The numerical and analytical results demonstrated strong agreement, highlighting the robustness of the XFEM approach for the analysis of cracked structures. This study aims to enhance the understanding of longitudinal crack initiation mechanisms in pipelines to facilitate the development of a proactive maintenance strategy that ensures their durability and reliability.

1. INTRODUCTION

Stainless steel 304 has long been used in the fabrication of pipelines for transporting energy resources in nuclear power plants. Given their critical function, ensuring the integrity of these pipelines is a primary concern, as environmental stresses can lead to structural defects, progressive material degradation, and ultimately, complete structural failure (Sanchez-Silva et al., 2011). Research has extensively focused on crack initiation and propagation mechanisms to minimize service interruptions and enhance pipeline reliability (Zheng et al., 2024). The stress intensity factor (SIF) is a key parameter used to evaluate material crack resistance, study elastic behavior, and define failure criteria. Simulation methods, such as the Finite Element Method (FEM) and Extended Finite Element Method (XFEM), have been widely employed in these investigations. For example, Okodi et al. (2020) explored the application of XFEM in Abaqus, utilizing maximum principal strain and energy release rate as damage parameters to analyze crack propagation and predict burst pressure. Bartaula et al. (2020) investigated oligocyclic fatigue in compact tension specimens and pipelines, assessing the limitations of fatigue analysis codes in Abaqus. Similarly, Montassir et al. (2020) examined semi-elliptical cracks in pipelines using XFEM to develop a failure evolution diagram, enhancing the understanding of defect progression. Additionally, Chen et al. (2020) coupled XFEM with hierarchical mesh adaptation and the direct method to model crack propagation, analyzing stress distribution at the crack tip and calculating the SIF. Lin et al., (2020) proposed a novel crack initiation criterion based on variable damage deformation at the crack tip.

Despite these advancements, the numerical modeling of rectangular cracks in pressurized pipes using XFEM in the elastic domain remains unexplored. This study aims to address this gap by applying XFEM to evaluate the effect of an external rectangular crack within the thickness of a pressurized tube. The results are compared with those from the literature obtained using the FEM approach.

2. MATERIALS AND METHODS

2.1. XFEM formulation

The findings from the literature on analyzing cracking in pressurized pipelines rely heavily on the application of the Finite Element Method (FEM). In this approach, the mesh must incorporate the crack, positioning it at the interfaces between mesh elements, with the crack tip corresponding to a mesh node (Alshoaibi et al., 2022). Near the crack tip, as analyzed by fracture mechanics, the stress field tends to infinity, a representation that can be physically debatable. However, from a mathematical standpoint, this implies a singularity in displacement, which typically hinders achieving optimal convergence rates for finite elements. To address this issue, researchers have adopted an approach involving the refinement and updating of the mesh around the crack tip. This remeshing operation proves costly and often difficult to control. To optimize the quality of solutions provided by finite elements, researchers introduced the Extended Finite Element Method (XFEM), which relies on a singular enrichment technique. For example, studies like those of Salmi et al. (2020b) investigating the effect of three-dimensional elliptical profile cracks on pipes with a double-slope transition using XFEM demonstrated that this approach is an effective tool for modeling cracks in pipes. Pioneering work by Babuska and Milenk laid the foundation, followed by researchers like Nash and Gifford and Alturi et al., who made modifications to the method, obtaining relevant results for stationary cracks. Further contributors like Méos, Benlytshko, and Dolbow have also enhanced the XFEM methodology with their research, thereby improving the quality of the proposed solutions. The fundamental principle of XFEM consists of integrating enrichment functions close to the expected solution into the function base used to approximate the problem (Merle & Dolbow, 2002).Within the XFEM the approximate local standard finite element approximation is enhanced in order to describe the locally enforced discontinuities With this the strains are handled particularly at a given node ($\boldsymbol{x_i}$), the approximation of displacement U is represented as follows (Rahman et al., 1998):

$$U(x) = \sum_i N_i\,(x)[U_1 + U(\alpha_i)a_i + (\sum_{k=1\to 4} \beta_k(x_i)b_{i,k}\,)] \tag{1}$$

Where: N −is the finite standard element (FE) shape function associated with node I,

U −represents the unknown displacement at node i in the standard FE formulation,

N is the set of all domain nodes N d ⊂ denotes the subset of nodes where the enrichment Heaviside function applied. This subset includes nodes that are located in elements completely intersected by the crack surface. We have (Lee & Martin, 2016):

$$\mathrm{H}\,(\mathrm{x}\,) = \begin{cases} 1 \text{ si } \varphi > 0 \\ -1 \text{ si } \varphi < 0 \end{cases} \tag{2}$$

Where : φ − is the normal level function,

a_i −is the unknown associated with the enrichment function H(x) at node I

For these specific nodes indicated in Fig. 1 with a square, the following equations hold true. Undefined, $N_P \subset N$ refers to the subset of nodes where the enrichment function β_j is applied, respectively for part of the elements only intersec by crack front. The crack tip is characterized using specific enrichment functions (Salmi et al., 2019):

$$\beta_j(x) = \{\sqrt{r}\sin(\tfrac{\theta}{2})\,\sqrt{r}\,\cos(\tfrac{\theta}{2}), \sqrt{r}\,\sin(\tfrac{\theta}{2})\,\sin(\theta), \sqrt{r}\,\cos(\tfrac{\theta}{2})\,\sin(\theta)\} \tag{3}$$

in which r=$\sqrt{(Q^2 + \Psi^2}$ and θ = $\tan^{-1}(\frac{Q}{\Psi})$ with Q and ψ are the normal and tangential level sets , those nodes are surrounded by circle in Figure 1.

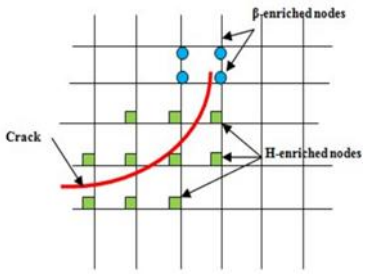

Fig. 1. The enrichment method in XFEM (Salmi et al., 2020a)

2.2. The theoretical computation of the stress intensity factor

The analysis of the behavior of cracked materials relies mainly on the principles of linear-elastic fracture mechanics. Using the literature, the approach used to address pipeline cracking problems is the Stress Intensity Factor (SIF), this gives an indication of the strength of the stress field at the extrimity of the crack. It is used to measure fracture in a material and varies with the stress that is put on the structure and the geometry of the structure. Raju also identified that the mode 1 stress intensity factor expression is (Raju & Newman, 1982):

$$K_1 = \frac{PR_i^2}{R_e^2 - R_i^2}\sqrt{\frac{\pi a}{Q}}\left[(2G_0 + 2G_1\left(\frac{a}{R_e}\right) + 3G_2\left(\frac{a}{R_e}\right)^2 + 4G_3\left(\frac{a}{R_e}\right)^3\right] \quad (4)$$

Where: $Q = 1 + 1{,}464\,(\frac{a}{c})^{1{,}65}$ for a/c < 1

with: R_i − inner radius,
R_e − Outer radius,
a − Crack depth,
P − Applied pressure inside the pipe,
Q − Shape factor,
c − Half-lenght of surface crack,
G_0,G_1,G_2, G_3 − Functions dependent on geometry of cylinder,

The expression for Stress Intensity Factor KI in a two-dimensional cracked plate is (El fakkoussi et al., 2018; Merle & Dolbow, 2002):

$$K_1 = \mathrm{F}\sigma\sqrt{\pi a} \quad (5)$$

Where:

$$F = \left[1{,}12 - 0{,}23\left(\frac{C}{L}\right) + 10{,}55\left(\frac{C}{L}\right)^2 - 21{,}72\left(\frac{C}{L}\right)^3 + 30{,}39\left(\frac{C}{L}\right)^4\right] \quad (6)$$

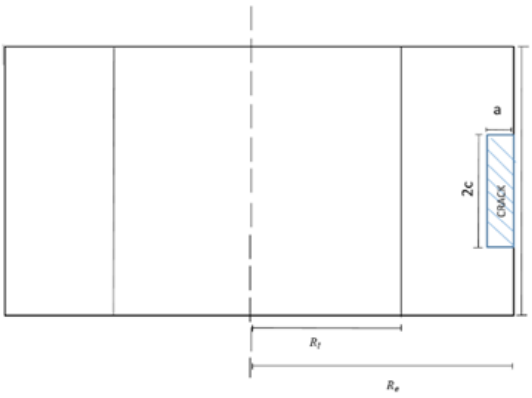

Fig. 2. Cylinder with an axial crack, shown in cross-section

2.3. Sif calculation using the XFEM method

The parameter G represents the energy dissipated for an infinitesimal crack advancement, while the G theta method is used to evaluate the J-integral in both elastic and plastic deformations. The J-integral, an analytical concept introduced by Cherepanov (1967), was demonstrated by Rice (1968) to be related to G in elastically dominated regions. This relationship is described by the stress intensity factor (SIF), where a point I is located on the crack front C. The crack surface, denoted as Γ_c is composed of an outer surface Γ_c^+ and an inner surface Γ_c^-. The volume V, which contains the crack front C (illustrated by the red arc in Figure 3) is defined by : $V = \Gamma_0 \cup \Gamma_1 \cup \Gamma_2 \cup \Gamma_c^+ \cup \Gamma_c^-$. Level set functions are employed as a regional reference at the fracture edge to characterize the location III throughout the volume V. Sukumar utilized the gradients of these level set functions to define this local basis (Fig. 5) as $e_1 = \nabla\Psi$, $e_2 = \nabla\phi$ and $e_3 = e_1 \times e_2$

within the framework of the XFEM, the J-integral is expressed within this local basis (Figure 4) defined by level set functions, and is given by the following equation (Moës et al., 2002):

$$J = \int_{\Gamma_c^+ \cup \Gamma_c^-} P_{lm}\, n_j \, d\Gamma - \int_V P_{lm,\theta} \, dV \tag{7}$$

P_{lm} is the Eshelby tensor defined by (1956):

$$P_{lm} = w\delta_{lm} - \sigma_{km}\, \varepsilon_{lk} \; (l, m, k) \in \{1,2,3\} \tag{8}$$

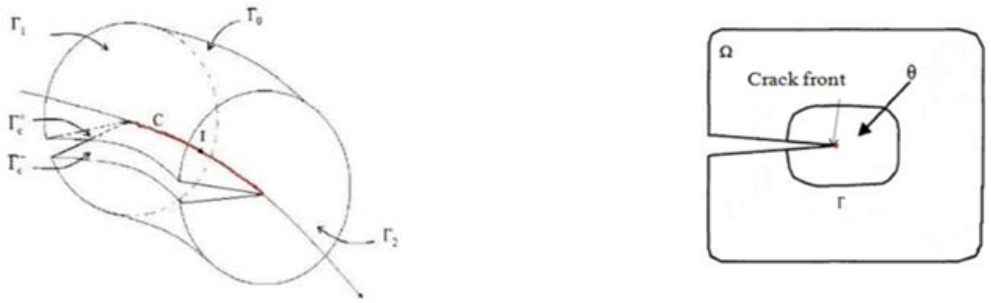

(a) **(b)**

Fig. 3. (a) The region V in J –integral; (b) Illustration of a θ distribution in a two- dimensional space (Salmi et al., 2020a)

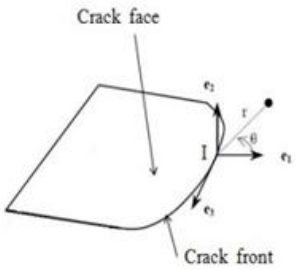

Fig. 4. Regional reference frame at the fracture edge (Salmi et al., 2020a)

With: $w-$ is the elastic energy density,

σ and ϵ $-$representing the stress and strain, respectively, in the basis (e_1, e_2, e_3) (Figure4),

θ $-$is a displacement field parallel to the crack plane and normal to the crack front (Fig. 3b), defined by:

$$\theta = \mu e_1 \;,\; \mu(I) = 1 \text{ and } \mu(x) = 0 \text{ for } x \in \Gamma_0 \cup \Gamma_1 \cup \Gamma_2 \tag{9}$$

For materials exhibiting elastic behavior, G can be derived from the J-integral using the follow equation (Merle & Dolbow, 2002):

$$G = \frac{E}{2(1-\upsilon^2)} \times \frac{J}{\int_c \mu dc} \quad (10)$$

The SIF is obtained from G using the follow equation (Merle & Dolbow, 2002):

$$G=\frac{K^2}{E'} \quad \text{Wit : } E' = \frac{E}{(1-\upsilon^2)} \quad \text{in plane strain} \quad (11)$$

2.4. Materials

The material studied in this work is 304 stainless steels, a common alloy in the austenitic stainless steel family, known for its chemical composition of iron, chromium and nickel, and its mechanical properties that make it more resistant to corrosion. This characteristic is the main reason for its use in pipeline structures, as these elements are exposed to corrosive environments. This type of material helps to extend the service life of pipelines (Tang et al., 2001; Azouggagh, 2018):

Fig. 5. Fracture of a pipe with longitudinal crack (Ministère du Développement durable, 2014)

Tab. 1. Chemical composition of material specimens (weight%) (Rogalski et al.,2020)

Fe	**Ni**	**Mn**	**Si**	**C**	**S**
20	10.24	1.56	0.41	0.014	0.008

Tab. 2. Mechanical properties of steel 30L (Azougagh., 2018)

Young's modulus	E= 198 GPa
Poisson's ratio	υ= 0.3
Yield stress	Re= 165 MPa
Ultimate tensil strenght	Rm= 240 MPa
Elongation to fracture	A= 35%

2.5. Numerical modeling

This study focuses on determining SIF in mode I by modeling the performance of a cylinder within the elastic domain using ABAQUS version 6.14 software. To evaluate the complete contour integral, Abaqus offers two different methods. The analysis utilized the XFEM method, in which the required information for the contour integral is self-determined based on the level set at a specific distance from the functions associated with the nodes of a given component (Lone et al., 2023).

The model examined in this study is a cylinder with a longitudinal rectangular crack extending to the outer surface. This choice was driven by the critical significance of such cracks in pressurized cylinders. Numerous researchers have investigated the behavior of pressurized pipelines with elliptical cracks using various numerical methods (Yu et al., 2023). However, the numerical modeling of rectangular cracks using the XFEM method in the elastic domain remains unexplored. The impact of parameters influencing crack initiation, such as its length, the type and magnitude of the applied load, and the mesh size used, was studied. The results of the SIF in mode I and the distribution of Von Mises stresses were extracted and compared to analytical and numerical values obtained from the classical method.

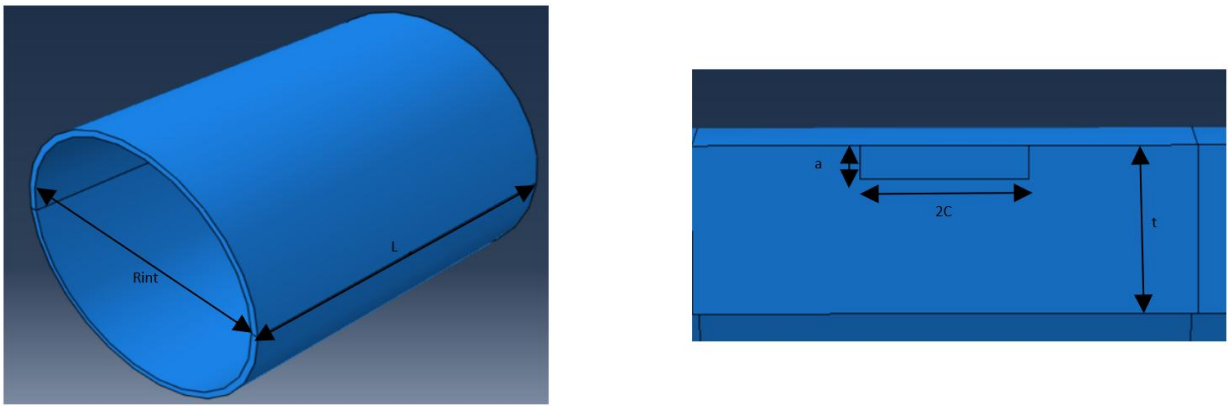

Fig. 6. Pipe and crack geometry

The cylinder is exposed to a constant amplitude internal pressure distributed across the walls of the finite element model, with its value defined according to the studied cases. For The boundary conditions used in this study are defined to prevent any displacement in the direction of the y-axis. The displacement, noted by u_y, is constrained to be zero across the entire surface of the cylinder (Eshelby, 1956),which is mathematically expressed as follows:

$$u_y(x, y, z) = 0 \text{ for } (x, y, z) \in \partial\Omega. \quad (12)$$

The dimensions of the pipline geometry adopted in this work are shown in table3 (Azougagh., 2018).

Tab. 3. Geometric characteristics of the pipe

Rint	193.2 mm
Rext	203.2 mm
Thickness (t)	10 mm
Lenght	500 mm

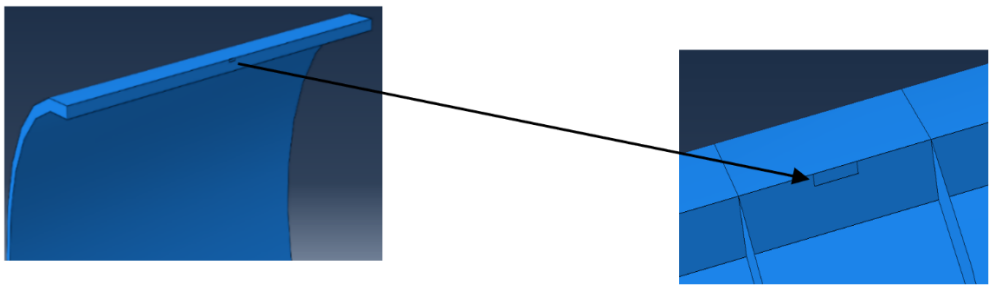

Fig. 7. Crack position in pipe geometry

2.6. Geometry meshing

Meshing in the XFEM is designed to present discontinuities, such as cracks, without requiring specific mesh refinement around them (Yu et al., 2023). Unlike the conventional in the finite element method, XFEM employs enriched shape functions that enable a crack to propagate through the elements by introducing additional degrees of freedom to the pertinent nodes. This approach captures singularities and crack openings without local mesh adjustments, thereby reducing computational costs. XFEM is particularly advantageous for complex geometries, where it avoids the challenges associated with creating a mesh that conforms to cracks (Xiao et al., 2021). Although a high-quality mesh can still enhance

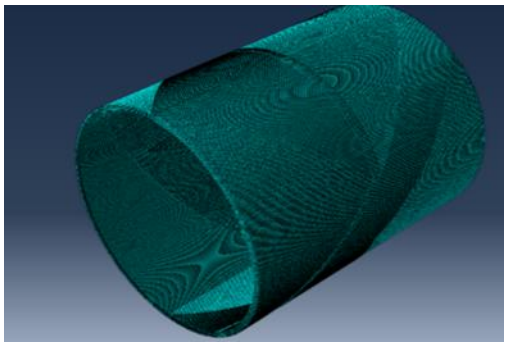

Fig. 8. Full tube meshing

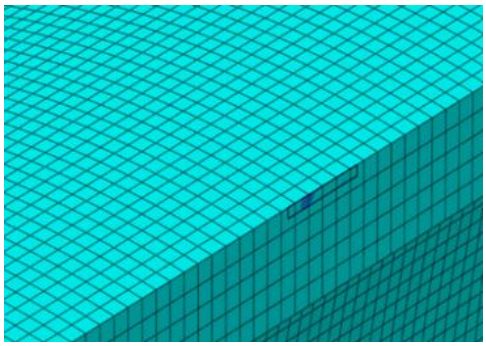

Fig. 9. Meshing of rectangular crack

To obtain precise and convergent results, the entire cylinder was modeled with a mesh of axisymmetric linear elements. We used 777,500 C3D8R elements with a size of 2 mm and 1,874,256 nodes. The mesh size was determined through testing conducted on a crack with an initial length of 1 mm, subjected to pressures of 10 MPa and 5 MPa. The mesh was refined and the number of elements increased. The results were analyzed for both pressure values. It was observed that the Von Mises stress increases with the number of elements, and SIF results converge towards analytical values for a mesh size of 2 mm.

Tab. 4. Von Mises stress for a =1 mm

P=5 MPa		**P=10 MPa**	
Number of elements	**Von-mises stress (MPa)**	**Number of elements**	**Von-mises stress (MPa)**
6200	104.9	6200	209.8
7728	104.6	7728	209.1
9828	104	9828	209.5
12638	104.4	12638	212.5
34362	118	34362	236.1
49600	125.4	49600	250.9
116625	140.3	116625	280.5
207414	152.1	207414	304.2
777500	168.5	777500	366.6

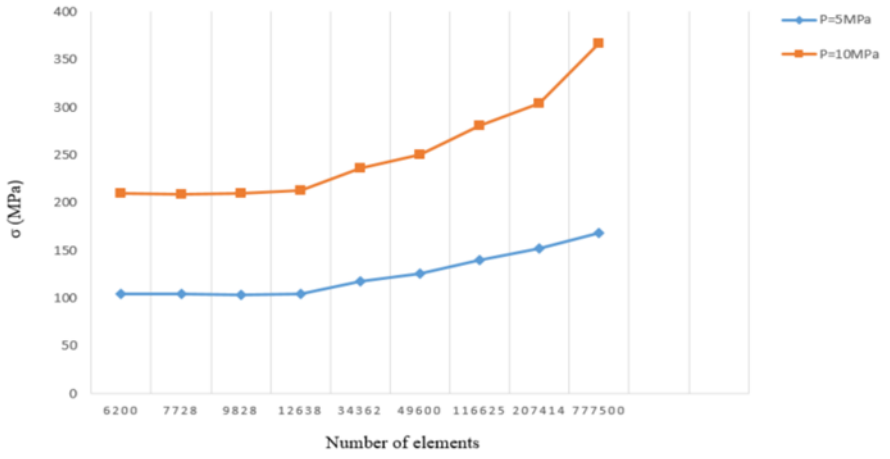

Fig. 10. Variation of Von Mises stress with the number of elements for a=1 mm

3. RESULTS AND DISCUSSION

3.1. Discussion of results

The Von Mises criterion, also referred to the distortion energy criterion, is crucial in materials science and engineering for assessing the failure of ductile materials. This criterion is based on the principle that a material's

failure is determined by the distortion energy rather than the total deformation energy. Mathematically, this criterion compares the distortion energy, represented by the Von Mises equivalent stress, to a critical threshold, usually the material's yield stress. The Von Mises stress is formulated based on the principal stresses of the material, and it is computed by means of the equation (Wang et al., 2021):

$$\sigma_{VM} = \sqrt{\frac{1}{2}[(\sigma_1 - \sigma_2)^2 + (\sigma_2 - \sigma_3)^2 + (\sigma_3 - \sigma_1)^2} \quad (13)$$

Material failure is anticipated when the Von Mises stress reaches or exceeds the yield stress, indicating the onset of plastic deformation.

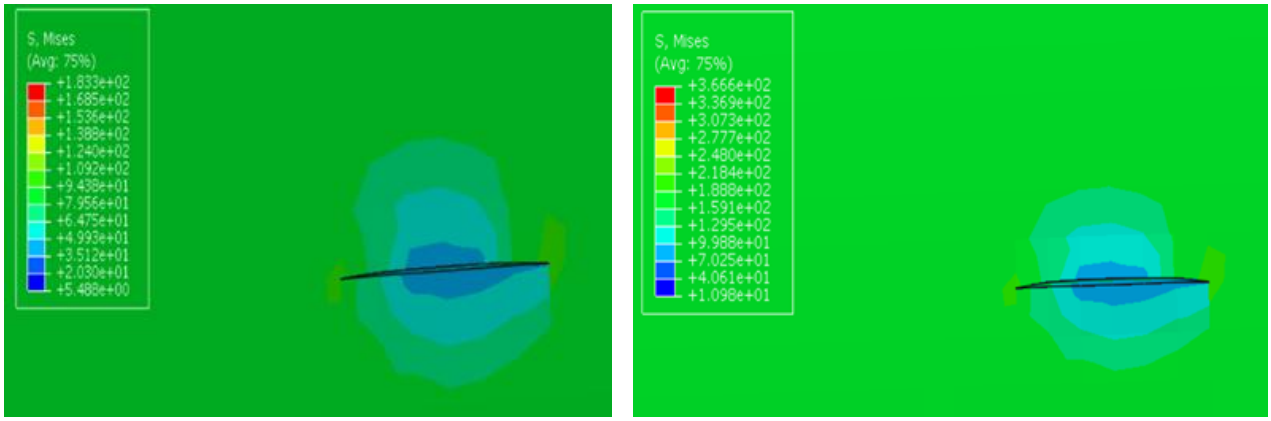

(a) **(b)**

Fig. 11. Von Mises stress distribution for a=1 mm with (a) P=5 MPa; (b) P=10 MPa

The use of the Von Mises criterion is commonly employed to evaluate stress states in isotropic materials (Xiao et al., 2021). This study presents an in-depth analysis of numerical results obtained using Abaqus software to evaluate the impact of initial crack length and applied pressure on the fatigue behavior of pipelines. Two initial crack lengths were considered (a=1 mm; a=2 mm), along with two levels of internal pressure (P=5MPa and P= 10 MPa). The evaluation of stress distribution was performed using the Von Mises criterion. The results reveal a marked concentration of stresses at the crack tips for both initial crack lengths. This concentration intensifies with increasing pressure, leading to a significant opening of the crack. When the pressure increases from 5 MPa to 10 MPa, the crack opening grows substantially due to the stress concentration, which amplifies the forces acting on the crack tips. For P=5 MPa, the maximum stresses remain below the material's yield strength, indicating the absence of plastic deformation. However, under a pressure of 10 MPa, the stress levels around the crack approach the yield strength (240 MPa), signaling a potential risk of structural failure. A comparison of the two initial crack lengths reveals that the crack opening is consistently larger for a=2 mm than for a=1 mm, regardless of the applied pressure. This highlights the critical role of the initial crack length in the structural behavior. The longer the crack, the greater the deformations caused by the applied pressure. These findings demonstrate that crack initiation and propagation in an elastic material strongly depend on the combined effects of the initial crack length and the applied load intensity.Furthermore, these results underscore that the initial crack length is a key parameter in determining the mechanical response of pipelines. Understanding the influence of these factors is essential for designing effective maintenance strategies and preventing catastrophic failures in pipelines subjected to cyclic loading conditions.

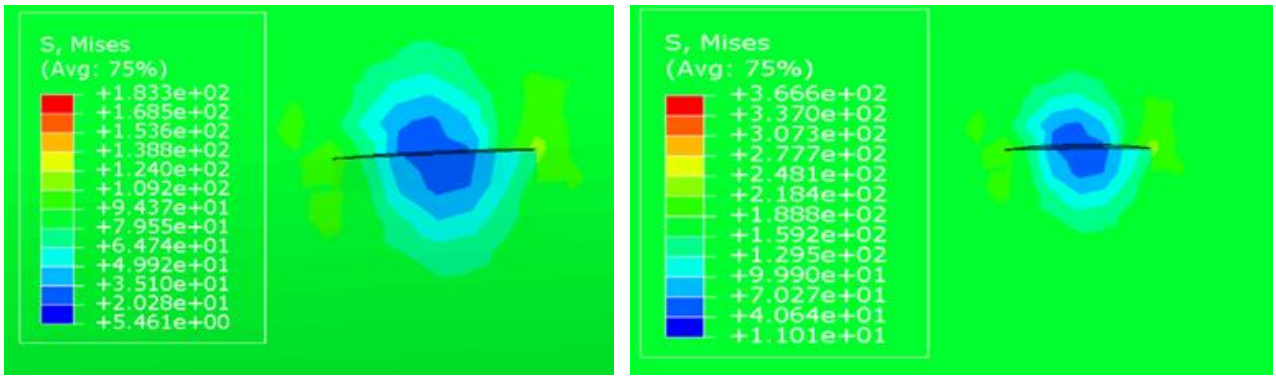

(a) **(b)**

Fig. 12. Von Mises stress distribution for a=2 mm with (a) P= 5 MPa; (b) P=10 MPa

The analysis indicates that stress concentration zones at the crack tips serve as the primary sites for plastic deformation and crack propagation. The increase in applied pressure exacerbates this phenomenon, reducing the load-bearing capacity of the structure and increasing the risk of failure. These findings also highlight that the initial crack length is a critical parameter in determining the mechanical response of pipelines.

The precise calculation of the stress intensity factor in mode I (K1) relies on the numerical model's ability to accurately capture the stress concentration at the crack tips. A sufficient number of contours and iterations is essential to ensure that the obtained K1 values are stable and independent of numerical choices. This study analyzes the evolution of K1 as a function of the number of contours and iterations for two pressure levels and two initial crack lengths. The results show that the K1 values converge starting from the fifth contour, which is located around the crack tip. The stability of the results is also influenced by the number of iterations, as demonstrated in the evolution curves presented in Figures 15 to 18.

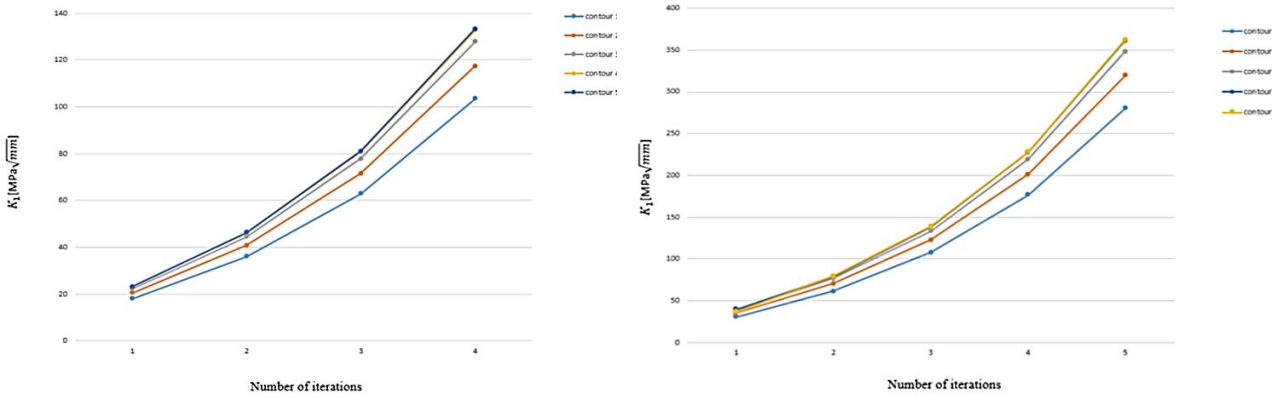

(a) **(b)**

Fig. 13. Evolution of SIF for each contour the based on the count of repetitions for (a) a=1 mm, P=5 MPa; (b) a=1 mm, P=10 MPa

The values of the stress intensity factor increase significantly for both crack lengths and applied pressures. This is explained by the ability of K1 to capture the intensity of stress concentration at the crack tip. Based on these results, it can be concluded that the stress intensity factor in mode I is a key parameter for describing the distribution of elastic stresses near the crack tips under normal opening. It is directly related to the concentration of stresses at the crack tips, where the stresses increase significantly due to the initial crack length and the applied loading conditions.

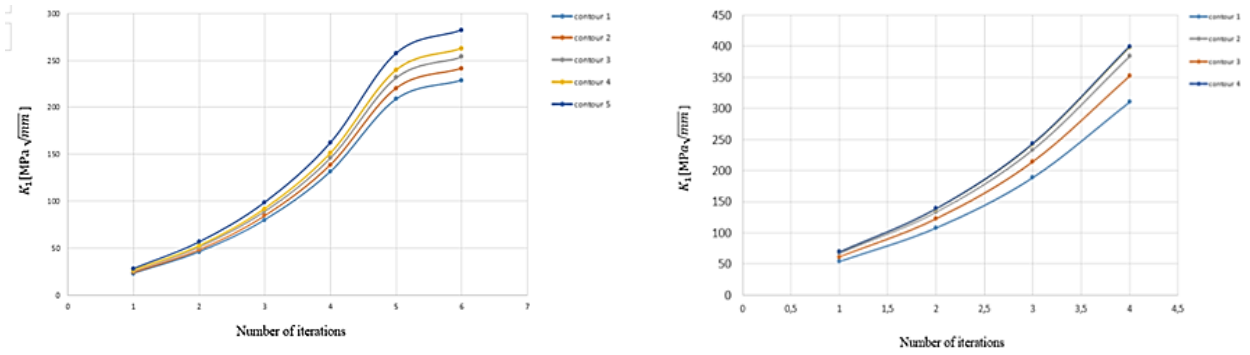

(a) **(b)**

Fig. 14. Evolution of SIF for each contour the based on the count of repetitions fo (a) a=2 mm, P=5 MPa; (b) a=2 mm, P=10 MPa

3.2. Comparison and validation

A detailed comparison was conducted between the results obtained through XFEM simulations and those derived from analytical calculations of the stress intensity factor (SIF) using Equations (5) and (6). The SIF values from XFEM simulations closely match the theoretical results, with an error margin not exceeding 1.6%. This low margin of error highlights the reliability of the XFEM approach in modeling cracked structures with high accuracy. Furthermore, validation of these results was performed by comparing them with the work of (Azougagh., 2018), who employed the classical FEM approach in his study. The disparity between the analytical and XFEM curves and the FEM curves, as depicted in Figures 23 and 24 for the two adopted values of crack length aaa, illustrates the limitations of the FEM method in addressing crack-related problems. These limitations stem from issues such as singularity at the crack tip and the requirement for repeated remeshing during crack propagation analysis. In contrast, the XFEM approach resolves these challenges by eliminating the need for remeshing and accurately capturing discontinuities. This capability results in more precise outcomes compared to both the classical FEM method and other damage models implemented in ABAQUS. Based on this comparison, it can be concluded that XFEM is the superior choice for accurately capturing crack growth. Its advantages lie in its ability to model crack propagation without remeshing and to represent discontinuities with a level of precision that surpasses classical FEM and other modeling approaches. This robustness makes XFEM an invaluable tool for analyzing complex fracture problems.

Tab. 5. Analytical and numerical results of SIF for a =1 mm

P (MPa)	FEM results (MPa$\sqrt{mm}$)	XFEM results(MPa$\sqrt{mm}$)	Theoretical results(MPa$\sqrt{mm}$)
5	56.92	181.1	191.76
10	110.67	383.3	383.53
15	170.76	544.1	575.29

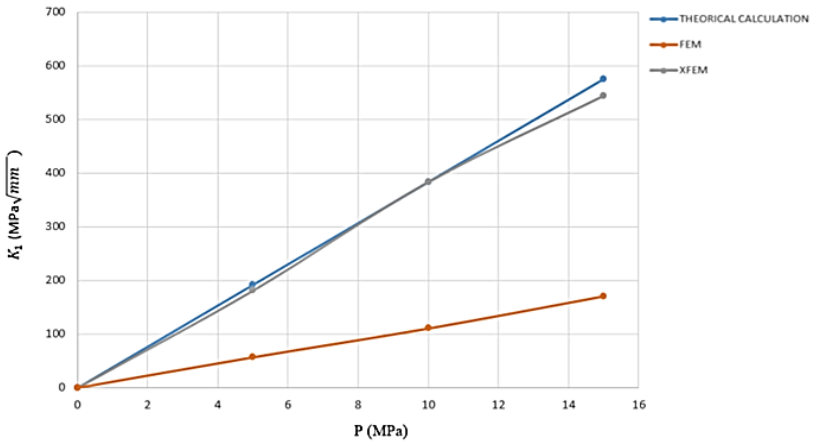

Fig. 15. Comparison of the variation of stress intensity factor for a=1 mm

Tab. 6. Analytical and numerical results of SIF for a =2 mm

P (MPa)	FEM results (MPa$\sqrt{mm}$)	XFEM results(MPa$\sqrt{mm}$)	Theoretical results(MPa$\sqrt{mm}$)
5	129.65	228.6	271.19
10	237.17	380.1	542.39
15	379.47	686.3	813.59

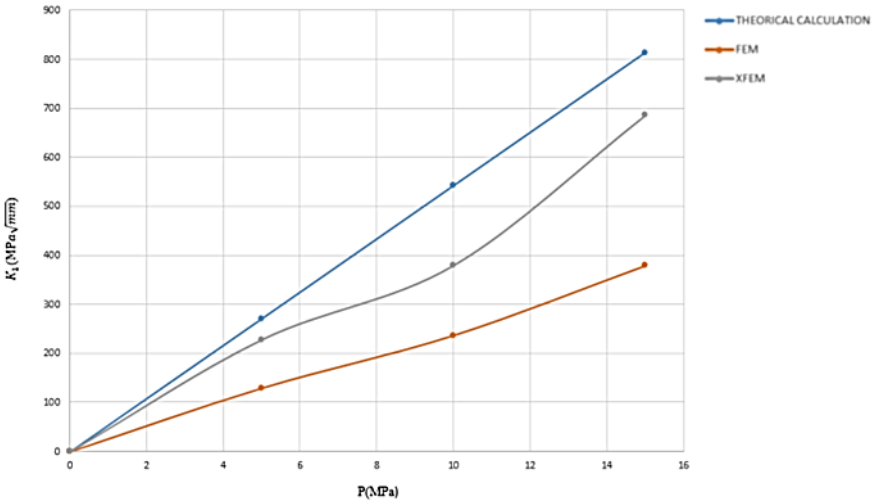

Fig. 16. Comparison of the variation of stress intensity factor for a=2mm

4. CONCLUSIONS

This study investigates the elastic behavior of a material containing a longitudinal rectangular crack embedded within the thickness of a pressurized tube. The study examines the effects of internal pressure, applied force, and initial crack length on the structural integrity of the tube. The Extended Finite Element Method (XFEM) was employed to effectively model the 3D rectangular crack problem using enrichment functions, enabling an accurate representation of the crack's geometry and behavior.

Initially, the distribution of Von Mises stress was analyzed for two initial crack lengths. The results revealed a significant stress concentration at the crack tips, leading to an increase in crack opening as the pressure increased. The analysis demonstrated that the tube becomes prone to failure when the applied pressure exceeds 5 MPa, emphasizing the critical role of stress amplification induced by the crack in compromising structural integrity. Subsequently, an analysis of the evolution of the Mode I Stress Intensity Factor (SIF) was conducted, showing that this parameter is a key measure for understanding the severity of cracks in materials. The impact of the number of contours and iterations in the XFEM simulation was also assessed, with the results confirming the SIF's capability to capture stress concentration accurately.

A comparative evaluation between theoretical, XFEM, and classical FEM results revealed strong agreement between the analytical values and those derived from the XFEM method, validating its reliability. Conversely, FEM results exhibited discrepancies due to limitations such as singularities at the crack tip and the necessity for remeshing, highlighting the advantages of XFEM in accurately and efficiently capturing crack behavior without these issues.

This study confirms the robustness and precision of the XFEM model for analyzing rectangular cracks in pressurized tubes. It also underscores the susceptibility of these tubes to plastic deformation when internal pressure exceeds 5 MPa, particularly near the crack tip. The findings provide a fundamental understanding of crack initiation mechanisms in pipelines, serving as a foundation for future investigations into the fatigue behavior of these structures. Future work will focus on analyzing defect propagation under critical loading conditions, enabling the prediction of pipeline lifespan and the development of proactive maintenance strategies to mitigate potential failures.

Author Contributions

Aya Barkaoui: Conceptualization, Methodology, Investigation, Writin. Mohammed el moussaid and Hassane moustabchir: Validation, Supervision, original draft

Conflicts of Interest

The authors declare no conflict of interest.

REFERENCES

Alshoaibi, A. M., & Fageehi, Y. A. (2022). A computational framework for 2D crack growth based on the adaptive finite element method. *Applied Sciences*, *13*(1), 284. https://doi.org/10.3390/app13010284

Azouggagh, M. (2018). Etude numerique de la propagation de fissure de fatigue dans l'acier inoxydable aust´enitique 304L. *Mémoire de thése doctorat d'université Moulay Ismail*.

Bartaula, D., Li, Y., Koduru, S., & Adeeb, S. (2020). Simulation of fatigue crack growth using XFEM. *Pressure Vessels and Piping Conference* (pp. V003T03A046). American Society of Mechanical Engineers. http://dx.doi.org/10.1115/PVP2020-21637

Chen, J., Zhou, X., Zhou, L., & Berto, F. (2020). Simple and effective approach to modeling crack propagation in the framework of extended finite element method. *Theoretical and Applied Fracture Mechanics*, *106*, 102452. https://doi.org/10.1016/j.tafmec.2019.102452

Cherepanov, G. P. (1967). The propagation of cracks in a continuous media. *Journal of Applied Mathematics and Mechanics*, *31*(3), 503-512. https://doi.org/10.1016/0021-8928(67)90034-2

El Fakkoussi, S., Moustabchir, H., Elkhalfi, A., & Pruncu, C. I. (2018). Application of the extended sogeometric analysis (X-IGA) to evaluate a pipeline structure containing an external crack. *Journal of Engineering*, *2018*(1), 4125765. https://doi.org/10.1155/2018/4125765

Eshelby, J. D. (1956). The continuum theory of lattice defects. *Solid State Physics*, *3*, 79-144. https://doi.org/10.1016/S0081-1947(08)60132-0

Lee, S., & Martin, D. (2016). Application of XFEM to model stationary crack and crack propagation for pressure containing subsea equipment. *Pressure Vessels and Piping Conference* (pp. V005T05A006). American Society of Mechanical Engineers. http://dx.doi.org/10.1115/PVP2016-63199

Lin, M., Li, Y., Salem, M., Cheng, J. R., Adeeb, S., & Kainat, M. (2020). A parametric study of variable crack initiation criterion in XFEM on pipeline steel. *Pressure Vessels and Piping Conference* (pp. PVP2020-21664). American Society of Mechanical Engineers. http://dx.doi.org/10.1115/PVP2020-21664

Lone, A. S., Harmain, G. A., & Jameel, A. (2023). Modeling of contact interfaces by penalty based enriched finite element method. *Mechanics of Advanced Materials and Structures*, 30(7), 1485-1503. https://doi.org/10.1080/15376494.2022.2034075

Merle, R., & Dolbow, J. (2002). Solving thermal and phase change problems with the extended finite element method. *Computational Mechanics*, *28*, 339-350. http://dx.doi.org/10.1007/s00466-002-0298-y

Ministère du Développement durable. (2014). *Rupture d'une canalisation de transport de pétrole brut*. https://www.aria.developpement-durable.gouv.fr/wp-content/files_mf/A45229_11fd_45229_stvigorddymonville_jfm.pdf

Moës, N., Gravouil, A., & Belytschko, T. (2002). Non-planar 3D crack growth by the extended finite element and level sets—Part I: Mechanical model. *International journal for numerical methods in engineering*, *53*(11), 2549-2568. https://doi.org/10.1002/nme.429

Montassir, S., Yakoubi, K., Moustabchir, H., Elkhalfi, A., Rajak, D. K., & Pruncu, C. I. (2020). Analysis of crack behaviour in pipeline system using FAD diagram based on numerical simulation under XFEM. *Applied Sciences*, *10*(17), 6129. https://doi.org/10.3390/app10176129

Okodi, A., Lin, M., Yoosef-Ghodsi, N., Kainat, M., Hassanien, S., & Adeeb, S. (2020). Crack propagation and burst pressure of longitudinally cracked pipelines using extended finite element method. *International Journal of Pressure Vessels and Piping*, *184*, 104115. https://doi.org/10.1016/j.ijpvp.2020.104115

Rahman, S., Ghadiali, N., Wilkowski, G. M., Moberg, F., & Brickstad, B. (1998). Crack-opening-area analyses for circumferential through-wall cracks in pipes—Part III: off-center cracks, restraint of bending, thickness transition and weld residual stresses. *International Journal of Pressure Vessels and Piping*, *75*(5), 397-415. https://doi.org/10.1016/S0308-0161(97)00083-5

Raju, I. S., & Newman Jr, J. C. (1982). Stress-intensity factors for internal and external surface cracks in cylindrical vessels. *Journal of Pressure Vessel Technology*, *104*. 293-298.

Rice, J. R. (1968). A path independent integral and the approximate analysis of strain concentration by notches and cracks. *Journal of Applied Mechanics*, *35*, 379-386.

Rogalski, G., Świerczyńska, A., Landowski, M., & Fydrych, D. (2020). Mechanical and microstructural characterization of TIG welded dissimilar joints between 304L austenitic stainless steel and Incoloy 800HT nickel alloy. *Metals*, *10*(5), 559. https://doi.org/10.3390/met10050559

Salmi, H., El Had, K., El Bhilat, H., & Hachim, A. (2019). Numerical analysis of the effect of external circumferential elliptical cracks in transition thickness zone of pressurized pipes using XFEM. *Journal of Applied and Computational Mechanics*, *5*(5), 861-874. http://dx.doi.org/10.22055/JACM.2019.28043.1452

Salmi, H., El Had, K., El Bhilat, H., & Hachim, A. (2020a). Numerical study of SIF for a crack in P265GH steel by XFEM. *Recent Advances in Mathematics and Technology: Proceedings of the First International Conference on Technology, Engineering, and Mathematics* (pp. 105-127). Springer International Publishing.

Salmi, H., Hachim, A., El Bhilat, H., & El Had, K. (2020b). Crack influence on a pipe with double slope under internal pressure: Numerical simulation with XFEM. *IIUM Engineering Journal*, 21(2), 266-283. http://dx.doi.org/10.31436/iiumej.v21i2.1454

Sanchez-Silva, M., Klutke, G. A., & Rosowsky, D. V. (2011). Life-cycle performance of structures subject to multiple deterioration mechanisms. *Structural Safety*, *33*(3), 206-217. http://dx.doi.org/10.1016/j.strusafe.2011.03.003

Tang, J. E., Halvarsson, M., Asteman, H., & Svensson, J. E. (2001). The microstructure of the base oxide on 304L steel. *Micron*, *32*(8), 799-805.

Wang, Y. Z., Li, G. Q., Wang, Y. B., & Lyu, Y. F. (2021). Simplified method to identify full von Mises stress-strain curve of structural metals. *Journal of Constructional Steel Research*, 181, 106624. https://doi.org/10.1016/j.jcsr.2021.106624

Xiao, G., Wen, L., & Tian, R. (2021). Arbitrary 3D crack propagation with Improved XFEM: Accurate and efficient crack geometries. *Computer Methods in Applied Mechanics and Engineering*, 377, 113659. https://doi.org/10.1016/j.cma.2020.113659

Yu, M. C., & Pan, W. F. (2023). Failure of elliptical tubes with different long–short axis ratios under cyclic bending in different directions. *Metals*, *13*(11), 1891. https://doi.org/10.3390/met13111891

Zheng, Y., Dong, Z., Zhang, X., & Shi, H. (2024). Pipeline reliability assessment and predictive maintenance considering multi-crack dependent degradation. *Journal of Engineering Manufacture*, *238*(8), 1122-1144. http://dx.doi.org/10.1177/09544054231190671